ELSEVIER

Polymer 43 (2002) 6955–6963

polymer

www.elsevier.com/locate/polymer

Poly(imide–amide)–poly(ethylene adipate) hybrid networks. II. Dielectric studies

A. Kanapitsas[a], P. Pissis[a,*], C.G. Delides[b], P. Sysel[c], V. Sindelar[c], V.A. Bershtein[d]

[a]*Department of Physics, National Technical University of Athens, Zografou Campus, 15780 Athens, Greece*
[b]*Laboratories of Physics and Materials Technology, Technological Education Institute (TEI) of Kozani, 50100 Kila, Kozani, Greece*
[c]*Department of Polymers, Institute of Chemical Technology, 5 Technicka, 16628 Praha 6, Czech Republic*
[d]*Ioffe Physico-Technical Institute of the Russian Academy of Sciences, 194021 St Petersburg, Russian Federation*

Abstract

Dielectric techniques, including thermally stimulated depolarization currents and isothermal discharging currents measurements in addition to classical dielectric relaxation spectroscopy, were employed to investigate molecular mobility in the poly(imide–amide)–poly(ethylene adipate) (PIA–PEA) hybrid materials with short ($M_n = 1.300$ g mol^{-1}) PEA crosslinks. The techniques used covered together the frequency range from 10^{-4} to 10^6 Hz. Secondary relaxations, the primary α relaxation of the PEA component, interfacial polarization and dc conductivity were studied. Significant reduction of the magnitude and broadening of the response is observed for the α relaxation of the PEA component in the hybrids. The results obtained have been analyzed in terms of morphological characterization. They suggest appearance of long-range connectivity of the PEA component in the hybrids at PEA contents between 60 and 70 wt%.

Keywords: Dielectric relaxation; Molecular mobility; Hybrid polymer networks

1. Introduction

In the first paper of the present series [1], SAXS, DSC and creep rate spectroscopy (CRS) techniques were employed to investigate nanometer-scale structure and segmental dynamics in PIA–PEA hybrid networks. Polymeric systems based on polyimides (PIs) are high-performance materials and find many applications, such as in microelectronics [2] and in membrane technologies [3]. In order to optimize synthesis and processing for preparing materials with predicted properties tailored to specific applications, a true understanding of the structure–property relationships is essential [4]. Dielectric techniques may provide significant contribution to the investigation of these relationships in polymeric systems [5], in synergy with other techniques, including SAXS, DSC and CRS.

In this second paper of the series, dielectric techniques are employed to investigate, over wide ranges of frequency and temperature, molecular mobility in the PIA–PEA hybrid networks with short PEA crosslinks ($M_n = 1.300 \times$ g mol^{-1}) of the previous paper [1]. Next to dielectric relaxation spectroscopy (DRS, 10^{-2}–10^6 Hz), mostly employed, the techniques used here include thermally stimulated depolarization currents (TSDC) and isothermal discharging currents (DC) measurements, which allow the extension of the frequency range covered down to 10^{-4} Hz. Moreover, TSDC is characterized by high sensitivity and high resolving power [6], which favor its use in studies on multicomponent systems.

In addition to the contribution to the investigation of the structure–property relationships, the dielectric techniques employed here provide the electrical and dielectric characterization of the PIA–PEA hybrid networks under study, which is essential for their potential use in microelectronics [2].

2. Experimental

2.1. Materials

The preparation of the materials has been described in the previous paper [1]. Next to pure linear PI and PEA network, the series of hybrid networks with short PEA crosslinks ($M_n = 1.300$ g mol^{-1}) and PIA/PEA weight ratios of 10/90, 20/80, 30/70, 40/60 and 80/20 were studied. The samples for dielectric measurements were in the form

* Corresponding author. Tel.: +30-1-7722986; fax: +30-1-7722932.
E-mail address: ppissis@central.ntua.gr (P. Pissis).

0032-3861/02/$ - see front matter
PII: S0032-3861(02)00666-3

of circular discs with evaporated silver electrodes on both surfaces.

2.2. Experimental techniques

For DRS measurements the complex dielectric permittivity, $\epsilon^* = \epsilon' - i\epsilon''$, was determined as a function of frequency (10^{-2}–10^6 Hz) in the temperature range from 130 to 350 K (controlled to better than ±0.1 K). A Schlumberger Frequency Response Analyzer (FRA SI 1260) supplemented by a buffer amplifier of variable gain (Chelsea Dielectric Interface) in combination with the Novocontrol Quatro Cryosytem were used.

For TSDC measurements the sample was inserted between the brass plates of a capacitor and polarized by the application of electric field E_p at temperature T_p for time t_p, which was large in comparison with the relaxation time at T_p of the dielectric dispersion under investigation. With the electric field still applied, the sample was cooled to temperature T_0 (which was sufficiently low to prevent depolarization by thermal excitation) and then was short-circuited and reheated at a constant rate b. A discharge current was generated as a function of temperature, which was measured with a sensitive electrometer (Keithley). The equivalent frequency f of TSDC measurements [6] spans $10^{-4} < f < 10^{-2}$ Hz. A common, home-made experimental apparatus [7] was used for TSDC measurements in the range 77–300 K. Typical experimental conditions were $E_p = 1$ MV/m for the polarizing field, $T_p = 295$ K for the polarization temperature, $t_p = 5$ min for the polarization time, 6 K/min for the cooling rate down to $T_0 = 77$ K, and 3 K/min for the heating rate.

For isothermal DC measurements, the TSDC apparatus was used. The polarization procedure and conditions were similar to those for TSDC measurements. The sample was then cooled at 6 K/min down to the temperature of measurements, where the electric field was removed, the sample was connected to the electrometer and the DC $I(t)$ was measured as a function of time. Fourier transform techniques or, alternatively, the Hamon approximation [8] were used for the calculation of the frequency dependence of dielectric loss, $\epsilon''(f)$, from the measured $I(t)$.

3. Results and discussion

3.1. The overall behavior

The overall dielectric behavior of all the samples studied, obtained by DRS measurements at room temperature (298 K) is shown in Fig. 1: real part of dielectric permittivity ϵ', dielectric losses ϵ'' and ac conductivity σ_{ac} as functions of frequency f. The conductivity σ_{ac} (actually the real part of the complex conductivity) has been calculated from the measured $\epsilon''(f)$ dependence by the equation

$$\sigma_{ac}(f) = \epsilon''(f)\epsilon_0 2\pi f \quad (1)$$

where ϵ_0 is the permittivity of free space. The rather high

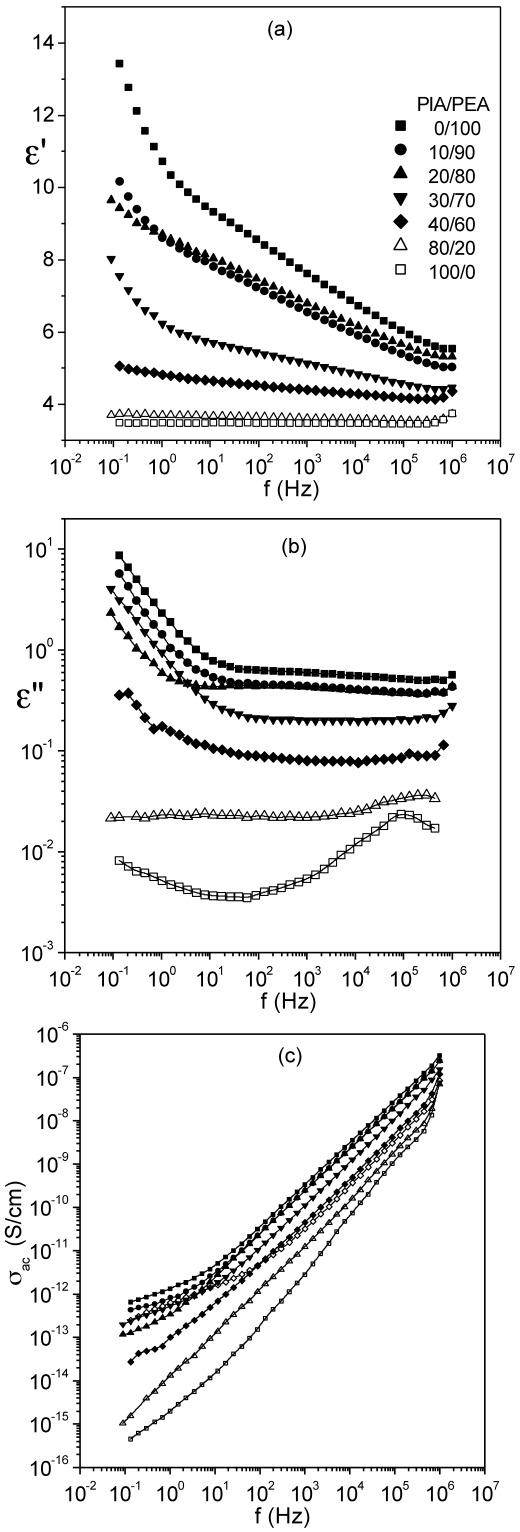

Fig. 1. Real part of dielectric permittivity ϵ' (a), dielectric losses ϵ'' (b) and ac conductivity σ_{ac} (c) against frequency f of the samples indicated on the plot at 298 K.

values of ϵ' and ϵ'' of the PEA-rich samples at low frequencies, increasing with decreasing frequency, are due to conductivity effects, as will be discussed in more detail later. The broad and weak loss peak of these PEA-rich samples in the kHz region and the corresponding decrease of ϵ' with increasing f are due to the α relaxation associated with the glass transition of the PEA component [9], as it should be expected also from the DSC data (Table 2 in Ref. [1]). The loss peak around 100 kHz in the PIA-rich samples is due to the secondary γ relaxation of PI [10,11].

On the basis of the overall dielectric behavior shown in Fig. 1 the samples can be classified basically into two groups: the PIA-rich samples (pure PI and 80 PIA–20 PEA) and the PEA-rich samples (pure PEA, 10 PIA–90 PEA, 20 PIA–80 PEA and 30 PIA–70 PEA). In the samples of the first group no conductivity effects are observed in the $\epsilon'(f)$ and $\epsilon''(f)$ plots and no tendency for a plateau at low frequencies in the $\sigma_{ac}(f)$ plot indicative of dc conductivity. The ϵ' values of the 80 PIA–20 PEA are only slightly larger than those of pure PI, e.g. 3.7 and 3.5 at 1 Hz, respectively. In the PEA-rich samples, on the other hand, conductivity effects in the $\epsilon'(f)$ and $\epsilon''(f)$ plots are rather strong, increasing with increasing PEA content, whereas a plateau is suggested in the $\sigma_{ac}(f)$ plot at low frequencies, as it will be confirmed by measurements at higher temperatures. The corresponding dc conductivity, σ_{dc}, increases with increasing PEA content. The behavior of the 40 PIA–60 PEA sample is intermediate regarding these two groups. This sample shows, in particular, increased values of ϵ' as compared to pure PI (by about 20% at 10 kHz) in combination with negligible conductivity effects.

The results reported above indicate long-range connectivity of the charge carrier conducting PEA component in the second group of samples and no such connectivity in the 80 PIA–20 PEA and the 40 PIA–60 PEA samples. Further support for that conclusion will be provided by the TSDC results. It is reasonable to correlate these results with those of permeability studies of organic vapors obtained with the same samples [3], as for the diffusion of both small molecules in permeability studies and ions in dielectric studies long-range connectivity of the flexible PEA component is needed. It was observed in Ref. [3] that the permeability of the 80 PIA–20 PEA and 50 PIA–50 PEA networks was similar to that of pure PI membranes and much smaller than that of membranes with higher PEA content. These results also suggest that both vapor permeability and ionic conductivity studies can be employed for morphological characterization, as the diffusing species probe the local morphology [12].

Fig. 2 shows comparative TSDC plots for the pure linear PI and PEA network and the 20 PIA–80 PEA and 80 PIA–20 PEA hybrids. Four peaks are observed in the pure PEA plot, designated as γ, β, α, and MWS in the order of increasing temperature. In agreement with previous TSDC studies on polyurethanes [9,12,13], including linear polyurethanes based on PEA [12], the γ and β peaks have been

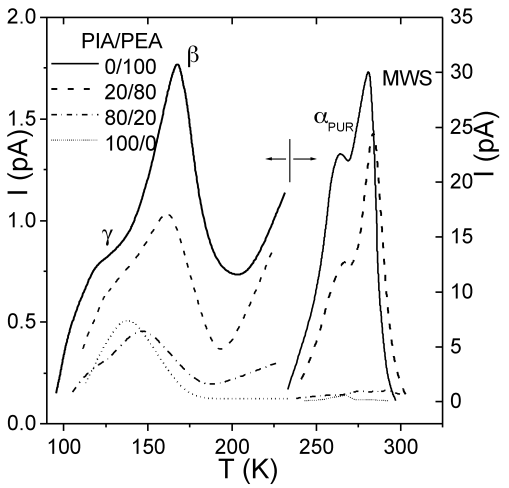

Fig. 2. TSDC thermograms of the samples indicated on the plot. The designation of the peaks refer to the PEA-rich samples. Please note the change of scale at about 230 K.

attributed to secondary relaxations associated with local motions of PEA chain segments. More precisely the γ peak has been associated with crankshaft motions of $(CH_2)_n$ sequences and the β peak to an association of adsorbed water molecules with polar carbonyl groups [12]. The α peak is located near to the calorimetric glass transition temperature T_g, determined in the previous paper [1], and arises from the reorientation of polar segments of PEA. Finally, the MWS peak, which is typical for polyurethanes of microphase-separated morphology, arises from the ionic polarization of Maxwell–Wagner–Sillars type (interfacial polarization) in the diffuse interphase boundary layer between hard and soft segment phase [13]. The TSDC plots of the 20 PIA–80 PEA hybrid in Fig. 2 and of the other PEA-rich samples not shown here are similar to that of the pure PEA network, with the magnitude of the peaks being reduced with decreasing PEA content (Table 1).

The TSDC plot of pure linear PI in Fig. 2 shows only one peak at about 140 K, in agreement with previous investigations [11,14]. This peak has been assigned to the secondary γ relaxation, associated with non-cooperative torsion vibrations of the imide cycles [10,15]. The γ peak of PI is much weaker than the secondary γ and β peaks of the pure PEA network in the same temperature region, as manifested in the TSDC plot of the 80 PIA–20 PEA network, which does not resemble that of pure PI.

The results obtained from the TSDC plots for all the samples are listed in Table 1. These include for each peak the temperature of current maximum and the current density maximum normalized to the same polarizing field and the same heating rate. The normalized current density maximum of a TSDC peak is a measure of the contribution $\Delta\epsilon$ of the corresponding relaxation mechanism to the static permittivity [6,7]. Included in Table 1 is ΔT_α, defined by $\Delta T_\alpha = T_\alpha - T_{1/2}$, where T_α is the peak temperature of the α peak and $T_{1/2}$ the temperature on the low-temperature side

Table 1
Temperatures T and normalized current density maxima J of the TSDC peaks for the samples under investigation. ΔT_α is the half-width of the TSDC α peak details in text

PIA/PEA weight ratio	T_γ (K)	T_β (K)	T_α (K)	T_{MWS} (K)	ΔT_α (K)	J_γ (10^{-9} A/m^2)	J_β (10^{-9} A/m^2)	J_α (10^{-9} A/m^2)	J_{MWS} (10^{-9} A/m^2)
0/100	120	166	263	280	10.0	5.5	11.4	16.9	24.8
10/90	123	162	263	279	11.5	4.7	7.6	13.2	22.6
20/80	120	160	266	283	13.0	3.7	7.2	9.8	20.2
30/70	116	160	258	279	12.5	2.9	5.5	5.0	19.6
40/60	123	152	255		18.0	2.6	4.2	1.9	(0)
80/20	123	146	(255)			3.1	4.8	(0.5)	(0)
0/100	138					4.0			(0)

of the peak, where the current has dropped to the half of its maximum value. ΔT_α is a measure of the distribution of relaxation times of the α relaxation [6,7], i.e. of the dynamic heterogeneity of segmental dynamics [1].

The results in Table 1 suggest that the secondary γ and β relaxations in the hybrid materials can be roughly described by a superposition of the relaxations in the pure components and deviations from that behavior are within experimental errors. The results are quite different in the high-temperature region of the α relaxation of the PEA component and the MWS interfacial polarization. There is a small shift in the α peak to lower temperatures in the middle compositions, which may be attributed, in agreement with conclusions drawn in the previous paper [1], to loosening of chain packing. On the other hand, the normalized current density maximum of the α peak, which is a measure of the contribution $\Delta\epsilon$ of the α relaxation to the static permittivity, decreases with decreasing PEA content much more faster than additivity would suggest. This result correlates well with the corresponding reduction of the heat capacity jump at T_g obtained by DSC with the same samples [1] and can be explained by constraining influence of the rigid PIA component on the softer PEA component due to anchoring of the PEA chain ends to the PIA chains. Finally, the manifestation of the increased dynamic heterogeneity of the segmental dynamics in the hybrids, observed in DSC/CRS measurements in the previous paper [1], is here the increased half-width of the TSDC α peak in the hybrids, as compared to the pure PEA network.

It is interesting to note, with respect to the α relaxation of the PEA component, that a very weak α peak is observed in the TSDC plot of the 80 PIA–20 PEA hybrid. This is not surprising, as TSDC is characterized by high sensitivity and, thus, capable of detecting very weak relaxations [6]. On the other hand, no multiple TSDC α peaks have been observed in the hybrids, corresponding to the multiple glass transitions observed by DSC in the previous paper [1]. Please note, however, that the TSDC α peak is accompanied by a strong interfacial MWS relaxation at higher temperatures, which would mask any additional, weak α peaks.

Deviations from additivity are even stronger for the interfacial MWS peak in Fig. 2 and Table 1 than for the α peak. This result should be expected, as the MWS peak reflects morphological properties at a larger spatial scale than the α peak. It is striking that the characteristics of the MWS peak listed in Table 1, peak temperature and normalized current density maximum, do not change significantly for the first four samples and that no well-defined MWS peak is observed for the last three samples. These results suggest a change of the morphology from one similar to that of pure PEA, i.e. characterized by long-range connectivity of the PEA component, in hybrids with 70% or more PEA to one with no such long-range connectivity in samples with 60% PEA or less. It is interesting but reasonable that the same classification of samples was done on the basis of conductivity effects observed in Fig. 1.

Fig. 3 shows the temperature dependence of dielectric losses ϵ'' at constant frequency of 1 kHz for selected PEA-rich samples. The measurements have been obtained isothermally, but they have been represented here in isochronal (constant frequency) plots to allow comparison with the TSDC plots of Fig. 2. The frequency have been selected rather high to suppress conductivity effects, which dominate the isothermal plots at low frequencies (Fig. 1). At low temperatures one broad secondary relaxation is

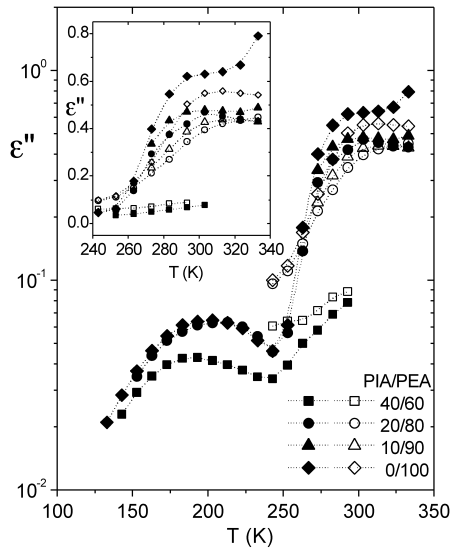

Fig. 3. Dielectric losses ϵ'' at 1 KHz (filled symbols) and at 100 KHz (open symbols) against temperature T for the samples indicated on the plot. The inset shows the same at high temperatures in a linear scale.

observed, very similar in the hybrids with 80 and 90% PEA and in the pure PEA network (please note, however, the logarithmic scale) and slightly faster (shifted to lower temperatures) in the 40 PIA–60 PEA hybrid. We remind that two overlapping secondary relaxations, γ and β in the order of increasing temperature, were obtained in these samples by TSDC (Fig. 2 and Table 1). This difference between DRS and TSDC measurements is discussed later.

At high temperatures conductivity effects dominate in Fig. 3 even at 1 kHz and mask the α relaxation of the PEA component. For that reason, data at a higher, second frequency, 100 kHz, have been included in Fig. 3 at the higher temperatures, whereas the inset shows the high-temperature region in a linear scale. The α relaxation is observed in these plots as a weak peak in the region 290–320 K, shifting to higher temperatures with increasing frequency and partly masked by conductivity.

3.2. The secondary relaxations

Fig. 4 shows the Arrhenius plot of the secondary γ relaxation in linear pure PI and in the hybrid with the lowest PEA content, 80 PIA–20 PEA. As indicated by the TSDC data in Table 1, the γ relaxation of the PIA component dominates over the secondary relaxations of the PEA component in this hybrid in the temperature region of the secondary relaxations. The experimental points in Fig. 4 have been obtained by DRS. Two more points obtained by TSDC have been included. Their coordinates are given by peak temperature T_γ (Table 1) and by the equivalent frequency [6] of 1.6 mHz, corresponding to a relaxation time τ of 100 s. Detailed comparison of DRS and TSDC data has indicated that $\tau = 100$ s is a reasonable value of the relaxation time at the temperature of a TSDC peak [6,7,16]. The inclusion of the TSDC points allows to expand the temperature and frequency range of data and, thus, to increase the accuracy of determination of the activation parameters.

The Arrhenius equation

$$f_{\max} = f_0 \exp\left(-\frac{E}{kT}\right) \tag{2}$$

where f_0 is the pre-exponential parameter, k the Boltzmann's constant, and E the apparent activation energy was fitted to the data. The best fittings give $E = 0.46$ eV and $f_0 = 10^{14}$ Hz for the linear PI and $E = 0.55$ eV, $f_0 = 10^{16}$ Hz for the 80 PIA–20 PEA hybrid. For comparison, we have determined the activation energy E of the linear PI also by TSDC, by following a special thermal sampling technique to isolate approximately single Debye responses in the central region of the relatively broad TSDC peak [6,7], and obtained $E = 0.45$ eV.

It is interesting to compare the values of activation energy E of the γ relaxation of linear PI, obtained here by DRS and TSDC, with those obtained for the same relaxation by similar techniques in other PI systems: $E = 0.43$ eV by DRS in two soluble PIs [15], $E = 0.45$ eV by TSDC in hybrid nanocomposites of PI and silica [17,18], $E = 0.49 - 0.54$ eV by DRS in several poly(amide–imide)s (PAIs) [10]. TSDC and dynamic mechanical analysis (DMA) measurements on the same PAIs as in Ref. [10] give E values in the range $0.48 - 0.55$ eV [19]. The relatively high and approximately similar values of E, obtained by various techniques in various PI systems, confirm the assignment of the γ relaxation to non-cooperative, localized motions of bulky groups common to all studied systems, such as imide cycles [10].

With respect to the inclusion of TSDC data together with DRS data in a common Arrhenius plot, it is important to confirm the common origin of the relaxations measured by the two techniques. This can be done also on the basis of the intensity (relaxation strength) of the relaxations studied. The current density maximum J_m (in A/m^2) of a TSDC peak has been shown to be related to the maximum of the dielectric loss ϵ''_m of the corresponding DRS loss peak by the equation [6]

$$\epsilon_0 \epsilon''_m E = 1.47 \frac{J_m}{2\pi f_m} \tag{3}$$

where E is the polarizing field in the TSDC experiment (in V/m), ϵ_0 the permittivity of free space, and f_m the equivalent frequency of TSDC measurements. With the data in Table 1 and $f_m = 1.6$ mHz, this equation gives for pure linear PI $\epsilon''_m = 0.047$, whereas the experimental value measured by DRS is equal to 0.038. Bearing in mind that the maximum of the dielectric loss in DRS experiments is also temperature-dependent, the agreement is rather good, providing support for the common origin of the two relaxations, in addition to that provided by Fig. 4.

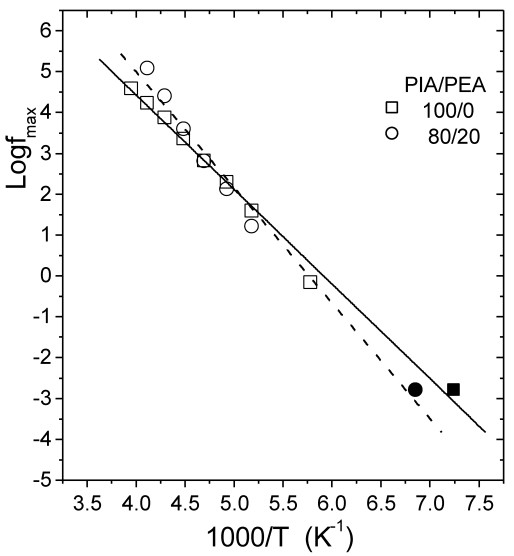

Fig. 4. Arrhenius plot of the secondary γ relaxation of the samples indicated on the plot. The full points have been obtained by TSDC.

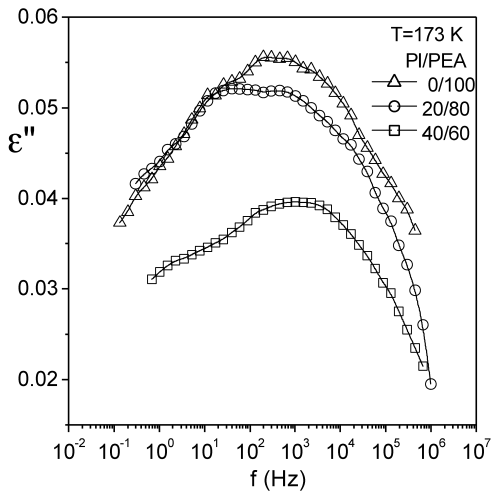

Fig. 5. Comparative plot of dielectric losses ϵ'' against frequency f of the PEA-rich samples indicated on the plot at 173 K.

So far to the secondary γ relaxation in the PIA-rich samples. Fig. 5 shows a comparative DRS plot of dielectric losses ϵ'' in PEA-rich samples at 173 K. A double loss peak is observed in each sample, corresponding to the two secondary TSDC peaks in Fig. 2 and in Table 1. The faster γ relaxation is located at lower temperatures in the isochronal (constant frequency) TSDC plots and at higher frequencies in the isothermal DRS plots, as compared to the slower β relaxation. It is striking that the γ relaxation is more intense than β in the DRS measurements, whereas the opposite is observed in the TSDC measurements. The explanation for that is as follows. In the equipment for DRS measurements the temperature of the sample is controlled by a nitrogen stream flowing through the sample cell. As a result of that the sample is dried, so that the β relaxation, which is assigned to an association of adsorbed water molecules with polar carbonyl groups [12], is reduced in magnitude. This hypothesis is in agreement with the results of previous dielectric measurements on polyurethanes containing different amounts of sorbed water [12] and has been confirmed by additional DRS and TSDC measurements on the samples of the present work at various levels of hydration.

To further check the assignment of the loss peaks in Fig. 5, the magnitude of the water content-independent γ relaxation measured in Fig. 5 has been compared with that calculated from the TSDC data in Table 1 by using Eq. (3). The measured values of ϵ''_{max} are 0.56, 0.51 and 0.39 for the samples with 100, 80 and 60% PEA content, respectively, whereas the corresponding calculated values are 0.63, 0.55 and 0.31. Bearing in mind uncertainties in the measured ϵ''_{max} values due to overlapping with the β relaxation in Fig. 5, the agreement is good enough to confirm that the low-temperature TSDC peaks in Fig. 2 has the same origin as the high-frequency DRS loss peak in Fig. 5, namely the γ relaxation.

The activation parameters of the γ relaxation of the PEA-rich samples, obtained from Arrhenius diagrams similar to that shown in Fig. 4, were found, within experimental errors, independent of composition, in consistency with constant temperature of the TSDC γ peak in Table 1 for these hybrids. The values of the activation parameters in Eq. (2), activation energy $E = 0.32$ eV and pre-exponential factor $f_0 = 4 \times 10^{12}$ Hz, are within the range of values determined by DRS and TSDC in polyurethane systems, e.g. 0.34 eV and 3×10^{11} Hz in polyurethanes based on polyoxypropylene glycol [16], 0.32 eV and 5×10^{13} Hz in polyurethanes based on oligotetramethylene glycol [13].

3.3. The primary α relaxation

The primary α or segmental relaxation associated with the glass transition of the PEA component was clearly observed as a TSDC peak in Fig. 2. As it is often the case in polyurethane systems, the α relaxation is to a large extent masked by conductivity effects in DRS measurements and, thus, difficult to study by DRS. It should be expected that α is more clearly observed in isothermal DC measurements, where, similar to TSDC, polarization and depolarization steps are isolated from each other and, thus, conductivity effects are suppressed. Fig. 6 shows $\epsilon''(f)$ for the pure PEA network calculated from DC measurements at 256 K, following the Hamon approximation [8]. The TSDC peak temperature T_α for that sample is 263 K (Table 1), as it is also the calorimetric glass transition temperature T_g [1]. A loss peak is observed in Fig. 6 at 2×10^{-3} Hz, which is out of the frequency range of DRS measurements in this work. In consistency with the TSDC and the DSC data, the peak is attributed to the α relaxation. Comparison with DRS data at the same temperature in the inset to Fig. 6 shows that the dipolar α loss peak cannot be observed by DRS in this temperature region as it is masked by conductivity.

The temperature region of the α relaxation (the glass transition) of the PEA component is indicated in the DRS

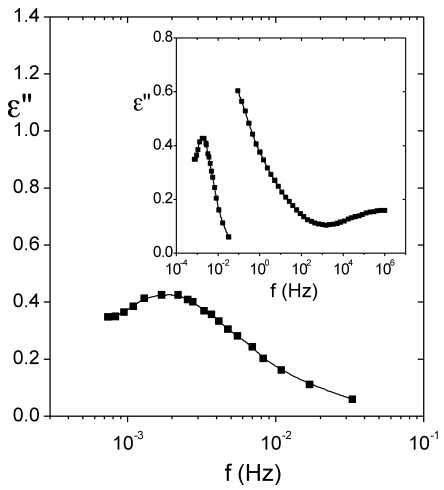

Fig. 6. Dielectric losses ϵ'' of the pure PEA network at low frequencies obtained by DC measurements at 256 K. The inset shows the same together with data obtained by DRS at higher frequencies.

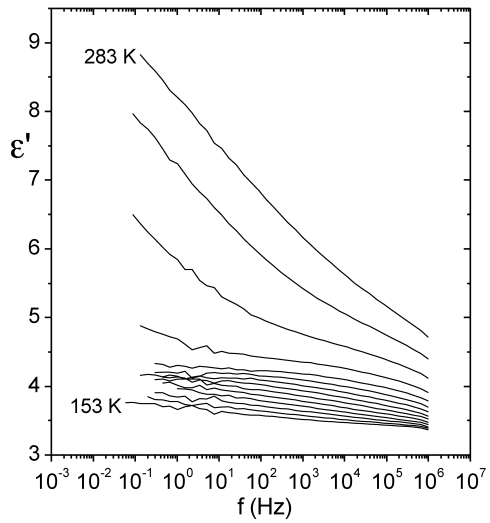

Fig. 7. Real part of dielectric permittivity ϵ' against frequency f in the 20 PIA–80 PEA hybrid at several temperatures between 153 and 283 K in steps of 10 K.

data of Fig. 7 showing ϵ' at several temperatures in the 20 PIA–80 PEA hybrid. At each frequency ϵ' increases with temperature in the glassy state reflecting the increase of molecular mobility. No conductivity effects, giving rise to increase of ϵ' at low frequencies, similar to that observed for the same hybrid in Fig. 1 at 298 K, are present at low temperatures. This changes at higher temperatures, and ϵ' clearly increases with decreasing frequency at low frequencies, starting with 263 K (or even 253 K), i.e. in the region of T_g.

Fig. 8 shows a comparative plot of tan $\delta = \epsilon''/\epsilon'$ for the PEA-rich samples in the region of the α relaxation at 283 K. The relaxations are more clearly observed in that representation, as conductivity effects, giving rise to increase of both ϵ' and ϵ'', are partly suppressed. The relaxations in Fig. 8 are not single. This should not be

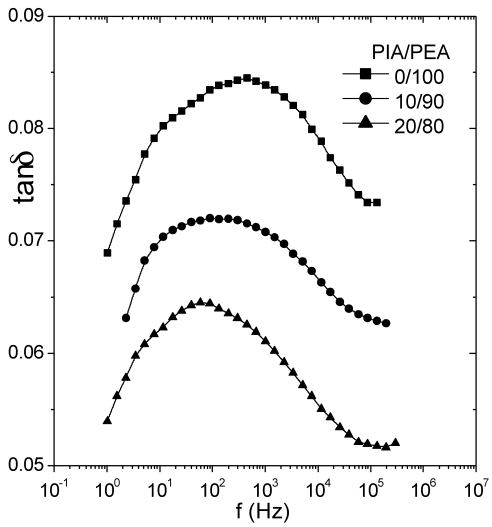

Fig. 8. Loss tangent, tan δ, against frequency f of the samples indicated on the plot at 283 K.

surprising, as PEA has a dipole moment aligned parallel to the chain contour, which gives rise to the so-called dielectric normal mode process [20]. The normal mode process (n relaxation) is related to the fluctiuation and orientation of the end-to-end polarization vector of the chain. The α relaxation and the n relaxation overlap with each other in the spectra of Fig. 8, as it is commonly observed in oligomers with molecular weight in the range of that of the short PEA crosslinks ($M_n = 1.300$ g mol^{-1}) of the present work [21, 22]. In agreement with the results of dielectric studies in other oligomers, the α relaxation in Fig. 8 is that at higher frequencies and the n relaxation that at lower frequencies. It is interesting to note that the n relaxation is observed in the PEA crosslinks, despite the fact that these are tethered from both ends to rigid constituents (PIA chains). A similar situation has been observed in poly(oxyethylene–oxybutylene–oxyethylene) (EBE) triblock copolymers, where B chains of $M_n = 970$ g mol^{-1} covalently bound to E chains at both ends exhibit n relaxation at temperatures where the E blocks are crystallized [22].

The dielectric spectra in Fig. 8 show, in agreement with but more clearly than those in Fig. 3, that in the region of the α relaxation of the PEA component the response of the hybrids decreases with decreasing PEA content more than it should correspond to additivity. This result is in agreement with the results of TSDC measurements in Fig. 2 and in Table 1 and with those of DSC and CRS measurements in the previous paper [1]. The reduction of segmental mobility of the PEA chains, observed in the two papers by thermal, mechanical and dielectric techniques, is explained by constraints to the motion of the PEA crosslinks imposed by the fixed ends.

The DSC and TSDC techniques, employed in the present and in the previous paper [1] to investigate the segmental dynamics of the PEA crosslinks, give for the glass transition temperature of the PEA component in the various hybrids, in agreement with each other, values in the range 255–268 K. Since these two techniques are characterized by approximately similar time scales (comparable heating rates), the agreement in their results suggest that they probe the mobility of molecular units of similar size [16].

3.4. Electrical conductivity

The results in Fig. 1 show that electrical conductivity in the hybrids decreases with decreasing PEA content. To quantify these results and utilize them for morphological characterization, the dc conductivity σ_{dc} of the PEA-rich samples was obtained at various temperatures from $\sigma_{ac}(f)$ plots similar to those shown in Fig. 1 as the value of σ_{ac} at 0.1 Hz. The values obtained by this procedure were used to construct the Arrhenius diagram shown in Fig. 9 for the samples with 100, 90 and 80% PEA. The results cannot be described by straight lines, corresponding to an Arrhenius equation similar to Eq. (2), which suggests that conductivity is governed by the motion of polymeric chains, as it has

Table 2
Parameters of the VTFH Eq. (4) for the dc conductivity σ_{dc}

PIA/PEA weight ratio	A (S/cm)	B (K)	T_0 (K)
0/100	6×10^{-6}	1450	199
10/90	1×10^{-6}	1555	185
20/80	1×10^{-6}	1726	187

often been observed in polymers at temperatures higher than T_g [13]. The Vogel–Tammann–Fulcher–Hesse (VTFH) equation [23–25]

$$\sigma_{dc} = A \exp\left(-\frac{B}{T - T_0}\right) \quad (4)$$

with temperature-independent, empirical parameters A, B, T_0, was used to describe the data. The fits were satisfactory and the values of fitting parameters are listed in Table 2. The Vogel temperature T_0 has been found in many polymers to be in the range of about 50 K below T_g, which is approximately the case also in the hybrids under investigation.

Ionic conductivity in polymeric systems can be employed for morphological characterization, as the motion of ions over macroscopic distances through the sample probe the local morphology [26]. The results in Fig. 9 and Table 2 suggest a long-range connectivity of the PEA component in the samples with 100, 90 and 80 wt% PEA, in agreement with the TSDC data in Table 1 and with the results of permeability measurements of organic vapors on the same samples [3].

4. Conclusions

Dielectric techniques, including TSDC and isothermal DC measurements in addition to classical DRS, were employed to investigate molecular mobility in the PIA–PEA hybrid materials with short ($M_n = 1.300$ g mol^{-1}) PEA crosslinks studied in the previous paper. The results obtained have been analyzed in terms of morphological characterization, and the following conclusions can be drawn:

1. Long-range connectivity of the PEA component is very clearly suggested by the characteristics of conductivity and of interfacial polarization in the materials with 70 wt% PEA or more, whereas materials with 60% PEA or less show no such connectivity.
2. In the temperature and frequency regions of the non-cooperative, local relaxations (γ and β in PEA, γ in PI) no significant deviations from additivity were observed. This refers to the temperature/frequency position of the relaxations, their magnitude and the activation parameters in the Arrhenius equation.
3. Significant reduction of the magnitude of the cooperative α relaxation, associated with the glass transition of the PEA component, in hybrids (by more than it would correspond to additivity) indicates suppression of segmental dynamics in the PEA crosslinks. At the same time, broadening of the response of the α relaxation indicates dynamic heterogeneity of segmental dynamics. These effects, in agreement with results obtained in the previous paper [1], are explained by constraints to segmental motion of the PEA crosslinks, imposed by the fixed chain ends on the rigid PIA chains.

It is interesting to note that deviations from additive behavior increase in the following order: for secondary relaxations, primary α (segmental) relaxation, and conductivity/interfacial polarization, i.e. with increasing characteristic length scale of the motional event.

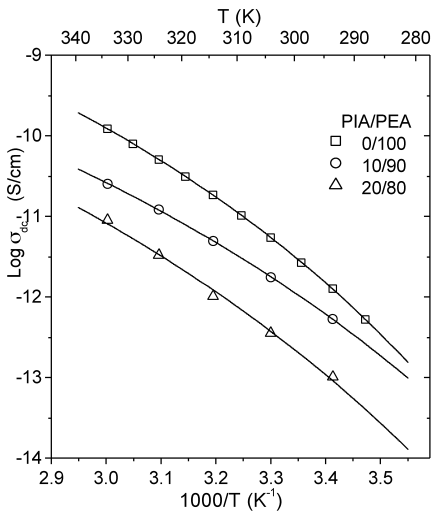

Fig. 9. Arrhenius diagram of the dc conductivity σ_{dc} of the samples indicated on the plot. The lines are best fit of the VTFH Eq. (4) to the data.

Acknowledgements

The authors are grateful to the Programme "Archimides" (ICS, NTUA), INTAS (project 97-1936), the Russian Fund for Basic Research (RFBR grant 00-03-33173), and NATO (PST.EV. 97310 grant for V.A.B.) for the financial support of this research.

References

[1] Bershtein VA, Egorov VM, Egorova LM, Yakushev PN, David L, Sysel P, Sindelar V, Pissis P. Polymer 2002;43:6943.
[2] Meier G. Progr Polym Sci 2001;26:3.
[3] Sindelar V, Sysel P, Hypnek V, Friess K, Sipek M, Castaneda N. Collect Czech Chem Commun 2001;66:533.
[4] Pissis P, Kyritsis A, Georgoussis G, Shilov V. Structure–property relationships in polyurethane ionomers. In: Nalwa HS, editor.

Advanced functional molecules and polymers. Synthesis, vol. 1. Amsterdam: Gordon and Breach Science; 2001. p. 317.
[5] Runt JP, Fitzgerald JJ, editors. Dielectric spectroscopy of polymeric materials. Washington, DC: American Chemical Society; 1997.
[6] van Turnhout J. Thermally stimulated discharge of electrets. In: Sessler GM, editor. Topics in applied physics. Electrets, vol. 33. Berlin: Springer; 1980. p. 81.
[7] Pissis P, Anagnostopoulou-Konsta A, Daoukaki-Diamanti D, Apekis L, Christodoulides C. J Non-Cryst Solids 1991;131–133:1174.
[8] Hamon BV. Proc Inst Electr Engr, Part IV 1952;27:151.
[9] Spathis G, Kontou E, Kefalas V, Apekis L, Christodoulides C, Pissis P, Ollivon M, Quinquenet S. J Macromol Sci, Phys B 1990;29:31.
[10] Stauga R, Schoenhals A, Carius H-E, Mudrak CV, Privalko VP. New Polym Mater 1998;5:119.
[11] Bershtein VA, Egorova LM, Yakushev PN, Meszaros O, Sysel P, David L, Kanapitsas A, Pissis P. J Macromol Sci, Phys B 2002;41:419.
[12] Pissis P, Apekis L, Christodoulides C, Niaounakis M, Kyritsis A, Jedbal J. J Polym Sci, Part B: Polym Phys 1996;34:1529.
[13] Pissis P, Kanapitsas A, Savelyev YuV, Akhranovich ER, Privalko EG, Privalko VP. Polymer 1998;39:3431.
[14] Bershtein VA, David L, Egorova LM, Kanapitsas A, Meszaros O, Pissis P, Sysel P, Jakushev PN. Mater Res Innovat 2002;5:230.
[15] Boiteux G, Oraison JM, Seytre G, Rabilland G, Sillion B. Soluble polyimides with specific dielectric behavior. In: Adabie MJM, Sillion B, editors. Polyimides and other high-temperature polymers. Amsterdam: Elsevier; 1991. p. 437.
[16] Vatalis AS, Kanapitsas A, Delides CG, Pissis P. Thermochim Acta 2001;372:33.
[17] Bershtein VA, Egorova LM, Yakushev PN, Georgoussis G, Kyritsis A, Pissis P, Sysel P, Brozova L. Macromol Symp 1999;146:9.
[18] Bershtein VA, Egorova LM, Yakushev PN, Georgoussis G, Kyritsis A, Pissis P, Sysel P, Brozova L. J Polym Sci, Part B: Polym Phys 2002;40:1056.
[19] Navio Peral N. Diploma thesis, Technical University of Valencia; 1998.
[20] Watanabe H, Yamada H, Urakowa O. Macromolecules 1995;28:6443.
[21] Schoenhals A. Macromolecules 1993;26:1309.
[22] Kyritsis A, Pissis P, Konsta A, Mai S-M, Booth C. IEEE Trans Diel Electr Insul 2000;7:509.
[23] Vogel H. Phys Z 1921;22:645.
[24] Fulcher GS. J Am Ceram Soc 1925;8:339.
[25] Tammann H, Hesse G. Z anorg Allg Chem 1926;156:245.
[26] Kanapitsas A, Pissis P, Kotsilkova R. J Non-Cryst Solids 2002;305:204.